NEW CRACK-TIP MODELS

G.P. Cherepanov*

The author's earlier theory of crack propagation in continua is modified accounting for special properties of the surface layer. Some new models of non-linear fracture mechanics are suggested, modeling the local plastic regions by slip lines. These are:

- the "Trident" model for long cracks,
- the "Octopus" model for short cracks,
- the "Martin" model for main cracks in gas pipe lines.

INTRODUCTION

The parameter governing the crack growth in continua is the Crack Tip Energy Flow Density (CTEFD) defined by an invariant integral along a small contour C enveloping the crack tip (Cherepanov (1), Williams (2), in a special case Rice (3)). This concept proved to be useful in practice as a criterion for crack initiation, provided contour C does not pass the non-proportional (plastic) process zone, Landes & Begley (4). The attempt to contract the contour C to the singular point O at the crack tip resulted in many cases in zero-CTEFD paradoxes which allowed only stepwise growth of cracks, Cherepanov (5). Moreover, the infinite deformation in the point O contradicts to trial, since the behaviour of any mechanical model for very large stresses and/or strains has no physical meaning. In what follows certain ways to overcome the paradoxes are briefly discussed. A more detailed treatment will be given somewhere else.

* Goncharova 8A, TOMILINO (Moscow Region)
140070 U.S.S.R.

A CONTINUUM COVERED BY A "SKIN"

Let us assume that all continuous media are similar to biological materials covered by a thin film or skin whose physical proporties are quite different from those at internal points. It is the skin which is responsible for the origin of surface micro cracks.
As a first approximation the skin will be modeled by a liquid non-separable film of zero thickness having a surface tension γ. On a traction free body surface S the skin stresses are:

$$\sigma_n = -\gamma/R, \quad \sigma_{nt} = 0 \tag{1}$$

where σ_n and σ_{nt} are the stresses normal and tangent to S, respectively, and R is the mean radius of curvature at the point under consideration. The value of γ for solids is equal to $10^{-2} \div 10^2$ N/cm, i.e. very small. Hence, the additional stresses caused by the skin can be ignored almost everywhere, except in a region of size Δ near the crack tip where the radius R is very small. In particular, certain cohesion forces arise between opposite borders of a crack whose magnitude and distribution are found from the solution of the boundary value problem (1). E.g., in the case of linear elastic materials, one can derive:

$$\Delta = \alpha_1 \gamma^2 K_I^{-2}, \quad \sigma_{max} = \beta_1 K_I^2 \gamma^{-1} \tag{2}$$

where:

α_1, β_1 = dimensionless parameters

K_I = stress intensity factor

σ_{max} = maximum stress at the crack-tip

For elastic-plastic materials equation (1) leads to $\Delta \approx \delta$, where δ is the crack opening displacement at the crack tip. Hence, we must use local finite deformations in this case in order to calculate cohesion forces.

Let a crack move with speed V in a continuum covered by skin. The stresses and strains near the crack tip may be considered as steady state in the moving coordinate system Ox_1x_2 (cf. figure 1). The calculation of the CTEFD, denoted by Γ, yields for this case, using the invariant integral of reference (1):

$$\Gamma = 2\gamma \cos\phi_A + {}_C\int \left[(U+T)n_1 - \sigma_{ij} n_j u_{i,1}\right] dC =$$

$$= \delta(W + a \rho V^2) + \gamma(2 \cos\phi_A + b) \qquad (i,j = 1,2) \tag{3}$$

where:

$W = \frac{1}{\delta} \int_S U \, dx_2$

$a = \frac{1}{2\delta} \int_S (u_{1,1}^2 + u_{2,1}^2) \, dx_2$

$b = \int_S u_{n,1} \, d\phi$

U = density of deformation work

T = density of kinetic energy

$\sigma_{i,j}$ = nominal (Piola-Kirchhoff) stresses

u_i = displacements

ρ = density

n_i = components of the unit normal to C

ϕ = inclination angle of the crack surface to the x_1-axis

δ = distance between A and B (integration on S is from A to B).

If irreversible deformations prior to failure are adequately modeled, the first term in equation (3) will be large compared to the others, so that equation (3) yields $\Gamma = \delta W$. The value of W strongly depends on the loading history prior to failure. E.g., the shaded area in figure 2 represents the quantity W, with the area of the loop being doubled.

If the deformations are approximated by those of an elastic solid, then equation (3) yields the well-known equation $\Gamma = 2\gamma$.

LONG CRACKS: THE TRIDENT MODEL

For long cracks the Trident model as depicted in figure 3 is of most interest. Local plastic deformations are modeled by certain systems of sliplines emanating from the crack tip:
For $\theta = \pm \alpha$ $0 < r < d_s$ (slip lines):

$$\sigma_{r\theta} = \tau_s, \; [\sigma_\theta] = 0, \; [u_\theta] = 0 \text{ for } \theta = 0, \; 0 < r < d_p \text{ (disclination):}$$

$$\sigma_\theta = \sigma_b, \; \sigma_{r\theta} = 0 \qquad (4)$$

where:

r, θ = polar coordinates

τ_s = yield stress in shear

σ_b = ultimate tensile stress

and square brackets denoting a jump of the quantity in brackets by crossing a discontinuity line.
The parameters d_s, d_p and α must be defined from the general maximum principle which requires the absolute maximum of the dissipation energy growth rate $\dot{D}$ (Cherepanov (6)):

$$\dot{D} = \frac{d}{dt} \left\{ 2\tau_s \int_0^{d_s} [u_r] \big|_{\theta=\alpha} dr + \sigma_b \int_0^{d_p} [u_\theta] \big|_{\theta=0} dr \right\} \qquad (5)$$

where t is the time or a loading parameter.
The Trident model is already well known in two limiting cases:

(i) when slip lines equal zero, i.e. $d_s = 0$, it corresponds to plane stress through-cracks in plates (Leonov & Panasiuk (7), Dugdale (8));

(ii) when disclination line equals zero, i.e. $d_p = 0$, it conforms to plane strain cracks (Cherepanov (9)).

Next, the basic modes of crack propagation in the framework of the trident model are discussed.

Steady state crack extension. Let the trident move without deformation. For this case the criterion parameter is the CTEFD, designated as Γ_0, with the integration path of the invariant integral enveloping the entire trident from O_1 to O_1'. The calculation yields:

$$\Gamma_0 = 2\Upsilon + 2\tau_s \delta_t + \sigma_b \delta_p + 2 \int_0^{d_s \cos\alpha} [U + T] \big|_{\theta=\alpha} dx_1 \qquad (6)$$

where:

δ_t = max $[u_r]$ on a slip line,

δ_p = max $[u_\theta]$ on the disclination.

The entire crack tip opening displacement in the Trident model equals $\delta_p + 2\delta_t \sin\alpha$.
This mode of crack extension corresponds to the concept of quasi-brittle fracture by Irwin and Orowan, with the Irwin's constant G_c for small scale yielding being equal to the value of Γ_0 in equation (6). Though the mode is unrealistic, it bridged a gap between the Griffith' theory and metals.

Unsteady crack extension. Let the slip lines and disclination of the trident grow simultaneously with crack extension. For this case the criterion parameter is the unsteady CTEFD, denoted by Γ_*, which is equal to (Cherepanov (10)):

$$\Gamma_* = \Gamma_0 + \dot{D} V^{-1} \tag{7}$$

This criterion allowed us to construct the theory of subcritical crack growth by arbitrary loading (in particular: cyclic) well verified by test data (10), (5).

Step-wise crack extension. According to this most realistic mode a crack starts very rapidly, with slip lines being absent and with the disclination developing during the jump. Slip lines grow only during the crack rest time. The criterion parameter of crack initiation and arrest is the CTEFD designated for this case as Γ_J, with the integration path of the invariant integral enveloping the disclination only with the fixed ends at the points O_2 and O_2' (cf. figure 3). The calculation results in:

$$\Gamma_J = 2\gamma + \delta_p \sigma_b \tag{8}$$

The critical and subcritical crack growth can be explained in the framework of the latter mode by introducing a certain characteristic structural distance which separates the neighbouring slip planes in a crystal. The slow stable crack growth is involved by the succesive shearing of these slip planes and breaking of bridges.

SHORT CRACKS: THE OCTOPUS MODEL

Let an edge plane-strain crack of length ℓ undergo the stretching load p (cf. figure 4). For very low loads, there grows self-similarly a plastic trident which is small as compared to ℓ:

$$d_p = \lambda p^2 \ell \tau_s^{-1} , \quad d_p/d_s = \text{constant} \tag{9}$$

where $p/\tau_s \ll 1$ and λ is a certain dimensionless coefficient.
Let us first calculate the value of Γ_J (with the integration path enveloping the front disclination) for fixed ℓ as a function of p. The chart of Γ_J in dimensionless variables is depicted in figure 5. For small scale yielding, when $p \to 0$ and $\gamma = 0$:

$$\Gamma_J = K_I^2 E^{-1} = 1.25 \pi p^2 \ell E^{-1} \tag{10}$$

where E is the Young's modulus.

With increasing p, two other slip lines directed to the free surfaces grow from the crack tip along the same slip planes: an octopus arises. The rising branch OA on figure 5 corresponds to the stable growth of four slip lines of the octopus. Then for a critical value of p the development becomes unstable, two slip lines fall to the free surface and a "plastic umbrella" appears, shutting the crack. At this point A, the magnitude Γ_J drops very rapidly. When increasing p further, the stable growth of the disclination and, especially, of the two front slip lines continues and the corresponding branch BD in figure 5 rises again.
Let us discuss the crack extension, as the simplest criterion utilizing the crack initiation condition:

$$\Gamma_J = \Gamma_c \tag{11}$$

Where Γ_c is a material constant (1).
According to figure 5 the crack does not extend under any loadings if $\ell < \Gamma_c/(\xi_D\sigma_b)$ (the phenomenon of non-propagating cracks). Here and below, ξ_A, ξ_B, ξ_D, ζ_0, ζ_B and ζ_1 are certain characteristic constants of the diagram in figure 5.
In the case of $\Gamma_c/(\xi_A\ \sigma_b) < \ell < \Gamma_c/(\xi_B\ \sigma_b)$, both extension and non-propagation of the crack are possible depending on load level. For loads in the range $\zeta_0 < p/\sigma_b < \zeta_B$ the crack can grow, because it does not have a plastic umbrella. The latter is available in the range of mean loads, when $\zeta_B < p/\sigma_b < \zeta_1$; this is the cause of crack non-propagation here. In the range of high loads, when $\zeta_1 < p/\sigma_b < 1$, the crack can extend in spite of the existence of the plastic umbrella (the phenomenon of arrest and temporary non-propagation of a crack). When $\ell > \Gamma_c/(\xi_B\sigma_b)$, the crack can grow by increasing load without forming the plastic umbrella and without stopping.

The phenomena mentioned are well known from experiments and explained exclusively by microstructural inhomogeneities in metals (cf. e.g. the recent paper by De Los Rios et al.(11)). The latter reason holds for any, including long, cracks.

With the plastic umbrella, the crack extension mechanism in the Octopus model implies the successive stepwise shearing of parallel slip lines and the motion of the crack by instant jumps due to breaking of bridges. The crack length increment per one jump equals some structural quantity $\Delta\ell$. E.g., for short microcracks in crystals the crack increases its length with $\Delta\ell = \eta a$ during one cycle of loading, where a is the interatomic distance, η is a certain number ($\eta = 1 \div 3$).

MAIN CRACKS IN GAS PIPE LINES: THE MARTIN MODEL

Let a crack in a cylindrical pipe of radius R_0 filled with gas under high pressure propagate with a constant speed V along a generatrix designated as the x-axis. The steady state propagation of the crack is possible only if $V \geq c$, where c is the sound velocity in gas. The active plastic and high moment stress regions form around the crack, approximately coinciding with one another. The regions of active and residual plastic deformations are double and single shaded in figure 6a, respectively. The shell buckles along the whole plastic region.
The pipe beyond the crack is considered elastic, with exception of the segments of discontinuous displacement $y = 0,\ 0 < x < d_p$ and $x = 0,\ |y| < d_s$, along which all active plastic deformations are concentrated (the Martin model, figure 6b). The front disclination is under stretching and bending. For $y = 0,\ 0 < x < d_p$:

$$\frac{N_y^2}{4h^2\,\sigma_s^2} + \frac{M_y}{h^2\,\sigma_s} = 1,\ N_{xy} = 0,\ M_{xy} = 0,\ [Q_y] = 0 \qquad (12)$$

where:

$N_x,\ N_y,\ N_{xy}$ = forces, $N_y = 2\sigma_s(h_1-h)$

$M_x,\ M_y,\ M_{xy}$ = moments of forces, $M_y = \sigma_s\, h_1(2h-h_1)$

$Q_x,\ Q_y$ = tearing forces

y = $R_0\ \psi$ (ψ is the angular coordinate)

$2h$ = shell thickness

σ_s = tensile yield stress

The diagram of the stress σ_y on the disclination is depicted in figure 6c, where z is normal to the shell. The shear, bending and twisting hold on slip lines, for $x = 0,\ 0 < |y| < d_s$:

$$\frac{N_{xy}^2}{4h^2\,\tau_s^2} + \frac{M_{xy}}{h^2\,\tau_s} = 1$$

$$[Q_x] = 0,\ [N_x] = [N_{xy}] = 0,\ [M_x] = [M_{xy}] = 0. \qquad (13)$$

with:

$N_{xy} = 2\tau_s(h_1-h),\quad M_{xy} = \sigma_s\, h_1(2h-h_1)$

The diagram of the stress τ_{xy} on the slip plane is similar to that of figure 6c.

The fracture controlling criterion is the invariant Γ-integral, the integration surface enveloping the disclination. It can be derived in the following form:

$$\Gamma = \int_C \int_{-h}^{+h} \left[(U+T)n_x - \sigma_{ij}\, n_j\, v_{i,x}\right] dC\, dZ + \iint_S p(x,y) \frac{\partial w}{\partial x}\, dx\, dy =$$

$$= 2 \int_0^{d_p} \int_{-h}^{+h} \left(\sigma_y \frac{\partial u_y}{\partial x}\right)\Big|_{y=0} dx\, dz =$$

$$= 2 \int_0^{d_p} \left\{N_y(x) \frac{du_{y0}}{dx} + M_y(x) \frac{du_{y1}}{dx}\right\} dx \qquad (14)$$

for: $y = 0,\ 0 < x < d_p:\ u_y = u_{y0}(x) + z\, u_{y1}(x)$

and $x = d_p:\ u_{y0} = u_{y1} = 0)$

where:

p = gas pressure
w = normal displacement of the shell
S = region enveloped by contour C.

Main cracks in gas pipelines were found to propagate by short successive jumps, crack initiation and arrest being controlled by the parameter Γ defined by equation (14).

CONCLUSION

The covered-by-skin solid model allows us:

(i) to do without singular stresses and strains near the crack-tip,
(ii) to correctly calculate the continuous crack growth in the framework of the CTEFD-concept by numerical procedures.

The emitted-slip-lines crack models are of practical importance for describing various effects of crack initiation, arrest and growth, in particular, relating to non-propagating short cracks.

REFERENCES

(1) Cherepanov, G.P., On propagation of cracks in continuous media. J.Appl. Math. & Mech (PMM), vol. 31, No. 3 (1967), pp. 476-488.

(2) Williams, M.L., On the mathematical criterion for fracture. In: Thin-Shell Structures, Prentice-Hall, Inc., Englewood Cliffs, New Yersey (1974), pp. 467-481.

(3) Rice, J.R., A path independent integral and the approximate analysis of strain concentration by notches and cracks. Trans. ASME, J. Appl. Mech., Vol. 35, No. 2 (1968), pp. 379-386.

(4) Landes, J.D., and J.A. Begley, The J-integral as a fracture criterion. In: Fracture Toughness, ASTM STP No. 514, Philadelphia (1972), pp. 1-23.

(5) Cherepanov, G.P., Mechanics of Brittle Fracture, McGraw Hill, New York (1979, Translation from Russian edition of 1974), pp. 950.

(6) Cherepanov, G.P., On the non-uniqueness problem in the theory of plasticity. Dokl. Akad. Nauk SSSR, Vol. 218, No. 4 (1974), pp. 779-782.

(7) Leonov, M.I., and V.V. Panasjuk, The development of cracks in solids. Appl. Mech. (PM), Vol. 5, No. 4 (1959), pp. 391-401 (in Ukrainian)

(8) Dugdale, D.S, Yielding of steel sheets containing slits. J. Mech. & Phys. Solids, Vol. 8, No. 2 (1960), pp. 100-104

(9) Cherepanov, G.P., Plastic slip lines at the crack-tip. J. Appl. Math.& Mech. (PMM), Vol. 40, No. 4 (1976), pp. 670-678.

(10) Cherepanov, G.P., On crack growth by cyclic loading. Appl. Mech. & Enging Physics (PMTF), No. 6 (1968), pp. 64-75.

(11) De Los Rios, E.R., Z.Tang and K.J. Miller, Short crack fatigue behaviour in a medium carbon steel. Fatique Engng. Mater. Struct., Vol.7, No. 2 (1984), pp. 97-108.

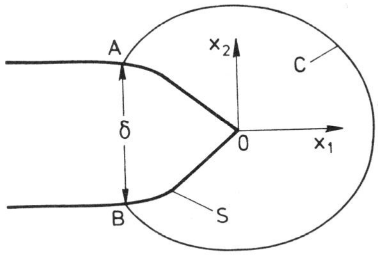

Figure 1 The crack tip vicinity in continua covered by a skin

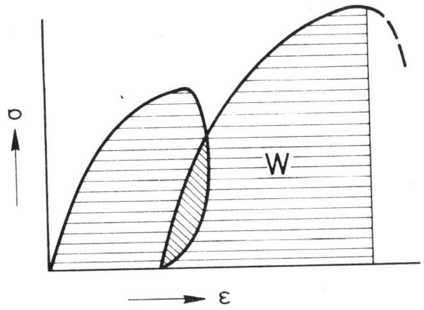

Figure 2 A σ-ε diagram illustrating a loading history of a particle in front of the crack tip

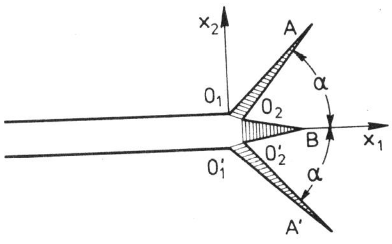

Figure 3 The Trident model for long cracks

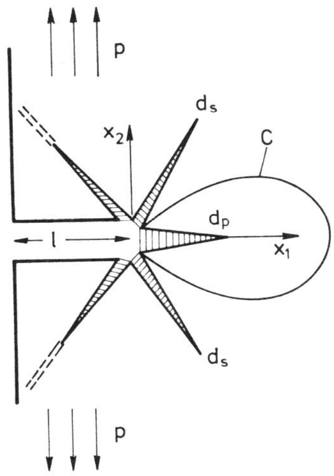

Figure 4 The Octopus model for short cracks

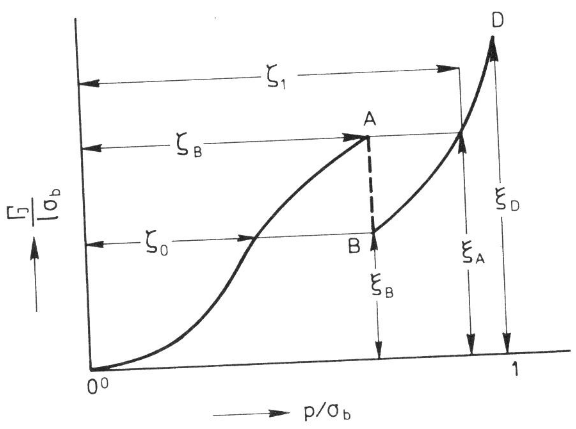

Figure 5 Diagram showing the fracture criterion Γ_J as a function of load p

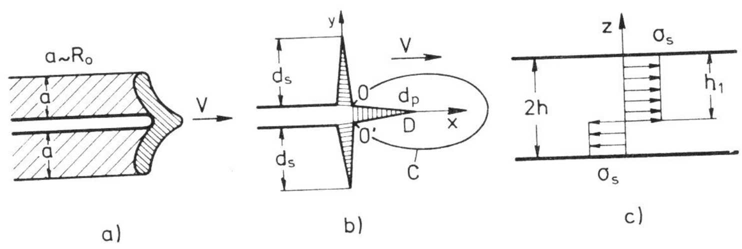

Figure 6 The Martin model for main cracks in gas pipe lines